

# Synthesis of magnetic chitosan supported metformin-Cu(II) complex as a recyclable catalyst for *N*-arylation of primary sulfonamides

Mahmoud Nasrollahzadeh\*, Zahra Nezafat, Khatereh Pakzad, Fatemeh Ahmadpoor

Department of Chemistry, Faculty of Science, University of Qom, Qom 37185-359, Iran



## ARTICLE INFO

### Article history:

Received 25 February 2021

Revised 17 May 2021

Accepted 30 May 2021

Available online 4 June 2021

### Keywords:

Sulfonamide

*N*-Arylation

Chitosan supported Cu(II) complex

Magnetic catalyst

Arylboronic acid

## ABSTRACT

The application of chitosan, which has received much attention as a natural polymer and effective support, has many advantages such as biodegradability and biocompatibility. In this study, the immobilization of a copper complex on the magnetic chitosan bearing metformin ligand has been developed through immobilizing structurally defined metformin with long tail of (3-chloropropyl)trimethoxysilane (TMOS). The synthesized  $\text{Fe}_3\text{O}_4$ -chitosan@metformin-Cu(II) complex ( $\text{Fe}_3\text{O}_4\text{-CS@Met-Cu(II)}$ ) was used as an effective, reusable and magnetic catalyst in the *N*-arylation of different derivatives of primary sulfonamides with arylboronic acids in ethanol. The primary sulfonamides were prepared from the reaction of sulfonyl chlorides with sodium cyanate in water under ultrasonic irradiation. Utilizing a wide variety of substrates in EtOH as a green solvent, high yields of the primary and secondary sulfonamides, easy work-up along with the excellent recovery and reusability of the catalyst, make this process a simple, economic and environmentally benign method. The synthesized  $\text{Fe}_3\text{O}_4\text{-CS@Met-Cu(II)}$  was characterized using various techniques such as XRD (X-ray diffraction), EDS (energy-dispersive X-ray spectroscopy), elemental mapping, TEM (transmission electron microscopy), FESEM (field emission scanning electron microscopy), VSM (vibrating sample magnetometer), ICP-MS (inductively coupled plasma mass spectroscopy), TGA (thermogravimetric analysis) and FT-IR (Fourier-transform infrared spectroscopy) analyses. The catalyst can be recycled and reused 5 times with no considerable loss of catalytic activity.

© 2021 Elsevier B.V. All rights reserved.

## 1. Introduction

Sulfonamides are a vital group of pharmaceutical compounds with an extensive spectrum of biological applications. In addition, they are applied as useful intermediates in organic synthesis. Sulfonamides with medicinal properties have various medicinal applications such as anticonvulsants and HIV protease inhibitors. Generally, sulfonamides are prepared via the reaction of sulfonyl chlorides with amine derivatives. Nevertheless, sulfonyl chlorides have some drawbacks, such as difficulty of handling and inappropriateness for long term storage. Only some of them are commercially available due to their instability [1–5].

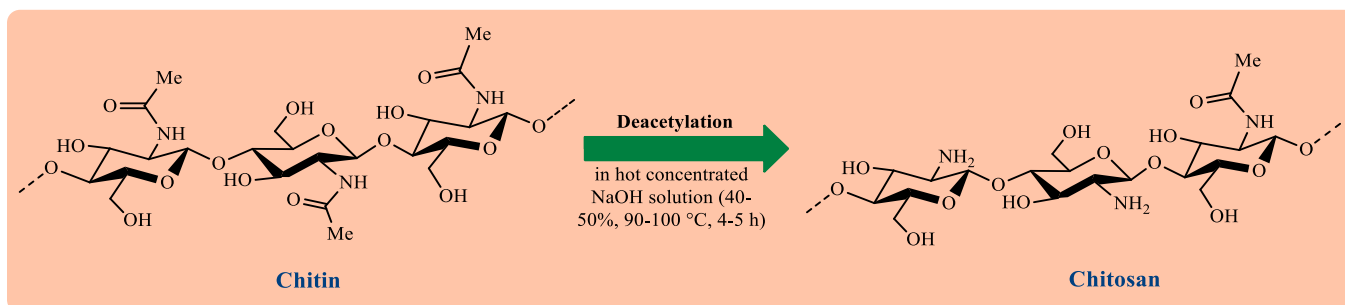
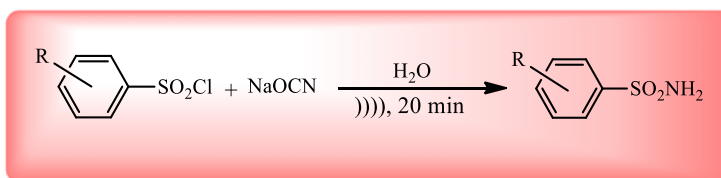
Usually, direct approaches are taken for the effective synthesis of *N*-aryl sulfonamides using various compounds such as aryl siloxanes, halides, boronic acids, etc., under diverse catalytic systems [6–10]. The use of palladium based catalysts is a known method for the synthesis of *N*-aryl sulfonamides [11,12]. The use of these catalysts is associated with problems; the most important of which

include high cost and toxicity. Therefore, researchers have tried to develop more efficient, cost effective, low toxicity and environmentally friendly catalysts for the synthesis of *N*-aryl sulfonamides. Copper based catalysts have been extremely effective for the synthesis of *N*-aryl sulfonamides from boronic acids and various primary sulfonamide derivatives. Copper based catalysts have some advantages, including high yield, low cost and non-toxic character [13–18].

Among various catalytic systems, heterogeneous catalysts are highly attractive for researchers because they have many advantages, the most important of which is the simple separation of the catalyst from the reaction mixture [19–22]. Therefore, one of the most important challenges in the preparation heterogeneous catalysts is the selection of the right support for the functionalization of metal nanoparticles (NPs) or complexes [23]. There are heterogeneous compounds, which are applied as efficient supports for the heterogenization of homogeneous catalysts via the decoration of homogeneous organometallic complexes, metal or metal oxide NPs on the their surface [24]. Different suitable supports must be used to synthesize heterogeneous catalysts such as graphene, natural and synthetic polymers [13,25–27], silicon dioxide, iron ox-

\* Corresponding author.

E-mail address: [mahmoudnasr81@gmail.com](mailto:mahmoudnasr81@gmail.com) (M. Nasrollahzadeh).

**Scheme 1.** Preparation of chitosan *via* deacetylation of chitin.**Scheme 2.** Synthesis of primary sulfonamides.

ide, MCM-41, poly(vinylidene fluoride), aluminum oxide, boehmite, SBA-15, etc. [28–36]. Among various supports,  $\text{Fe}_3\text{O}_4$  NPs are applied in electronic devices and biomedicine and as catalysts in different kinds of organic reactions due to their non-toxicity and superparamagnetic behavior, which allows their easy separation from the reaction media [37–39].

Presently, the use of natural polymers as efficient supports has received much attention. Among various biopolymers, chitosan has been very attractive [40–45]. Chitosan is a linear natural polymer glucosamine units, which is prepared from deacetylation of chitin in an alkaline environment (**Scheme 1**). Chitin is obtained from the exoskeleton of squids, crabs and shrimps. Chitosan has some advantages, including biodegradability, non-toxicity, biocompatibility, accessibility and pharmacological properties [46,47]. Chitosan is applied in various fields such as medicine and pharmacy due to its many benefits. It has biological properties such as antifungal, antibacterial, antioxidant and antitumor. In addition, chitosan is used as a suitable support for the preparation of various heterogeneous catalysts due to the suitable functional groups in its structure [48–51].

Nowadays, metal complexes have received much attention in various applications; especially in catalysis. Among the various atoms, nitrogen is the most widely used electron donor in ligand systems [52]. Metformin (Met) is one of the compounds used as an effective ligand [53–55].

In the present work, first, the synthesis of primary sulfonamides using sulfonyl chlorides and sodium cyanate under ultrasonic irradiation is reported (**Scheme 2**). Chitosan has then been used an efficient, novel and green support for the synthesis of a magnetic heterogeneous catalyst. In this regard, the metformin-copper(II) complex was immobilized on the  $\text{Fe}_3\text{O}_4$ -CS surface using (3-chloropropyl)trimethoxysilane (TMOS) (**Scheme 3**). The synthesized  $\text{Fe}_3\text{O}_4$ -CS@Met-Cu(II) was used in the *N*-arylation of primary sulfonamides as a novel and magnetic catalyst using arylboronic acids in ethanol solvent (**Scheme 4**).

## 2. Experimental

### 2.1. Tools and reagents

All chemicals were purchased from the Merck and Aldrich Chemical Co. and used with no additional purification. Chitosan

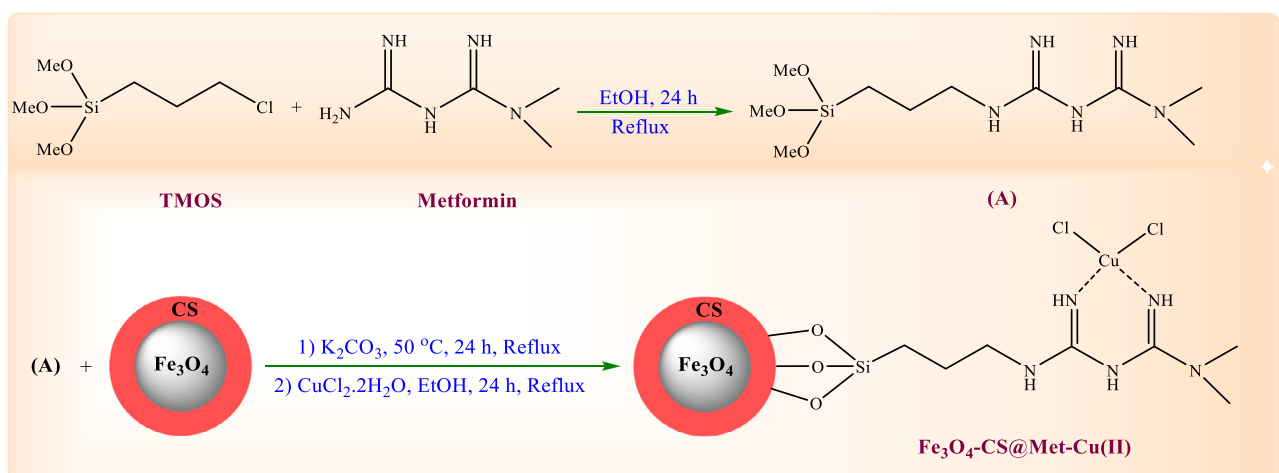
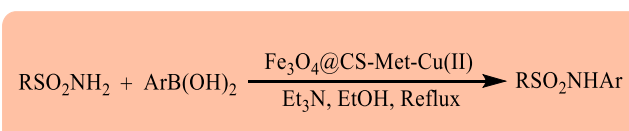
(De-acetylation degree: 85%, molecular weight: 50000–80000 Da (medium), particle dimension: powder with a mesh size of 80 (soluble in 1% acetic acid) was obtained from Nano Novin Polymer Co. The as-synthesized  $\text{Fe}_3\text{O}_4$  NPs supplied by Iran's Pishgaman-e Nano Mavad Co. were spherically shaped with particle sizes of approximately 20 nm. The synthesized compounds were characterized using FT-IR, NMR, XRD, TEM, TGA/DTG, VSM, EDS, elemental mapping, ICP-MS and FESEM. FT-IR and NMR spectra were recorded using Perkin-Elmer 781 and Bruker Avance DRX400 instruments, respectively. The magnetic property of the prepared complex was studied using VSM (Meghnatis Daghigh Kavir Co.) at 298 K. TEM and FESEM analyses were applied to evaluate the morphology of the catalyst using Philips CM120 and Cam scan Mv2300 instruments, respectively. XRD was conducted in the  $2\theta$  range of 10–80° using a Philips PW 1373 diffractometer ( $\text{Cu K}\alpha = 1.5406 \text{ \AA}$ ). TGA experiments were performed in the air flow at a heating rate of 10°/min using a TG 209F3 NETZSCH instrument. The elemental contents of the catalysts were determined by inductively coupled plasma optical emission spectrometry (ICP-MS, Perkin Elmer, Optima 8000)

### 2.2. Synthesis of $\text{Fe}_3\text{O}_4$ -Chitosan

$\text{Fe}_3\text{O}_4$ -Chitosan ( $\text{Fe}_3\text{O}_4$ -CS) was synthesized according to a literature method [56]. For this purpose, 0.25 g of CS in was dissolved 50 mL of 1% acetic acid (V/V), followed by the addition of 2 g of  $\text{Fe}_3\text{O}_4$  NPs and stirring for 0.5 h. In the final step, 50 mL of NaOH solution (1.0 M) were added slowly. The prepared  $\text{Fe}_3\text{O}_4$ -CS was collected by an external magnet.

### 2.3. Synthesis of $\text{Fe}_3\text{O}_4$ -Chitosan@Metformin-Cu(II) complex

Firstly, 5 mmol of metformin were added to 5 mmol of (3-chloropropyl)trimethoxysilane in EtOH (60 mL) and the mixture thus obtained was stirred under reflux conditions for 24 h (Solution A). Afterwards, 1.5 g of  $\text{Fe}_3\text{O}_4$ -CS in 70 mL of ethanol was subjected to ultrasonication for 20 min. 5 mmol of  $\text{K}_2\text{CO}_3$  were then added dropwise into the mixture of  $\text{Fe}_3\text{O}_4$ -CS and solution A, which was then refluxed for 24 h. Finally, the desired  $\text{Fe}_3\text{O}_4$ -CS@Met was collected using an external magnet, washed with ethanol, and dried at 60 °C in a vacuum oven for 12 h. In the next step, 1 g of the prepared  $\text{Fe}_3\text{O}_4$ -CS@Met in the previous step and

**Scheme 3.** Schematic representation of the synthesis of  $\text{Fe}_3\text{O}_4\text{-CS@Met-Cu(II)}$ .**Scheme 4.** N-Arylation of primary sulfonamides by phenylboronic acids using  $\text{Fe}_3\text{O}_4\text{-CS@Met-Cu(II)}$ .

0.5 g of  $\text{CuCl}_2\cdot 2\text{H}_2\text{O}$  were stirred under reflux conditions in 70 mL of ethanol for 24 h. Upon completion of the reaction, the synthesized magnetic catalyst was collected using a magnet, washed with ethanol, and dried (Scheme 3).

#### 2.4. Synthesis of primary sulfonamides

10 mmol of sodium cyanate ( $\text{NaOCN}$ ), 10 mmol of sulfonyl chloride, and 50 mL of distilled water were irradiated in an ultrasonic bath for 20 min. After completion of the reaction (monitored using TLC), the mixture was cooled and the pure white needle-shaped crystals were filtered [57].

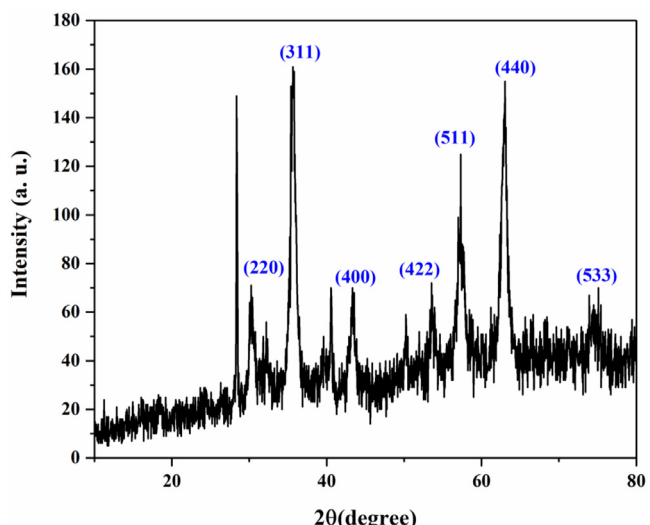
#### 2.5. N-Arylation of primary sulfonamides using $\text{Fe}_3\text{O}_4\text{-CS@Met-Cu(II)}$ catalyst

A 50 mL flask was filled with 0.5 mmol of primary sulfonamide, 0.5 mmol of arylboronic acid, 0.7 mmol of trimethylamine ( $\text{Et}_3\text{N}$ ), 0.02 g of  $\text{Fe}_3\text{O}_4\text{-CS@Met-Cu(II)}$ , and 7 mL of ethanol and the mixture thus obtained was stirred at reflux for the appropriate time (monitored using TLC). When the reaction was over, the reaction mixture was cooled and the catalyst was collected using an external magnet. After evaporation of ethanol, the solid residue was purified by recrystallization from ethyl acetate and n-hexane to yield the appropriate product. The melting points of products matched those reported in our previous work and literature values [13,57].

### 3. Results and discussion

#### 3.1. $\text{Fe}_3\text{O}_4\text{-CS@Met-Cu(II)}$ characterization

The synthesized  $\text{Fe}_3\text{O}_4\text{-CS@Met-Cu(II)}$  magnetic nanocatalyst was characterized using XRD, EDS, elemental mapping, FESEM, TEM, VSM, ICP-MS, TGA/DTG, and FT-IR spectroscopy.

**Fig. 1.** XRD pattern of  $\text{Fe}_3\text{O}_4\text{-CS@Met-Cu(II)}$ .

**Fig. 1** displays the XRD analysis of  $\text{Fe}_3\text{O}_4\text{-CS@Met-Cu(II)}$  magnetic nanocatalyst. The peaks with  $2\theta$  values of 30.3°, 35.9°, 43.4°, 54.0°, 57.3°, 63.2°, and 73.95 planes of the cubic  $\text{Fe}_3\text{O}_4$  (JCPDS 19-0629) confirm the presence of  $\text{Fe}_3\text{O}_4$  NPs [21].

EDS spectrum and elemental mapping were applied to study the chemical composition of the  $\text{Fe}_3\text{O}_4\text{-CS@Met}$  and  $\text{Fe}_3\text{O}_4\text{-CS@Met-Cu(II)}$  (Fig. 2 (a, b)). As shown in Fig. 2a, the presence of Fe, N, Si, O, and C elements in the  $\text{Fe}_3\text{O}_4\text{-CS@Met}$  structure is verified using EDS and elemental mapping analyses. As displayed in Fig. 2a, copper is not observed in the  $\text{Fe}_3\text{O}_4\text{-CS@Met}$  elemental mapping. According to the EDS and elemental mapping of the  $\text{Fe}_3\text{O}_4\text{-CS@Met-Cu(II)}$ , the presence of Fe, N, Si, O, Cu and C were confirmed in the structure of  $\text{Fe}_3\text{O}_4\text{-CS@Met-Cu(II)}$  (Fig. 2b). The content of the Cu within  $\text{Fe}_3\text{O}_4\text{-CS@Met-Cu(II)}$ , as determined using ICP-MS, was 9.1 wt. %.

FESEM and TEM analyses illustrated the morphology and particle size of  $\text{Fe}_3\text{O}_4\text{-CS@Met-Cu(II)}$  (Fig. 3). The results of FE-SEM display the spherical shape and uniform distribution of the particles in the nanometer range. The shape and size of the particles were investigated using TEM analysis (Fig. 3). As shown in Fig. 3, the morphology of the magnetic nanocatalyst is spherical, the average

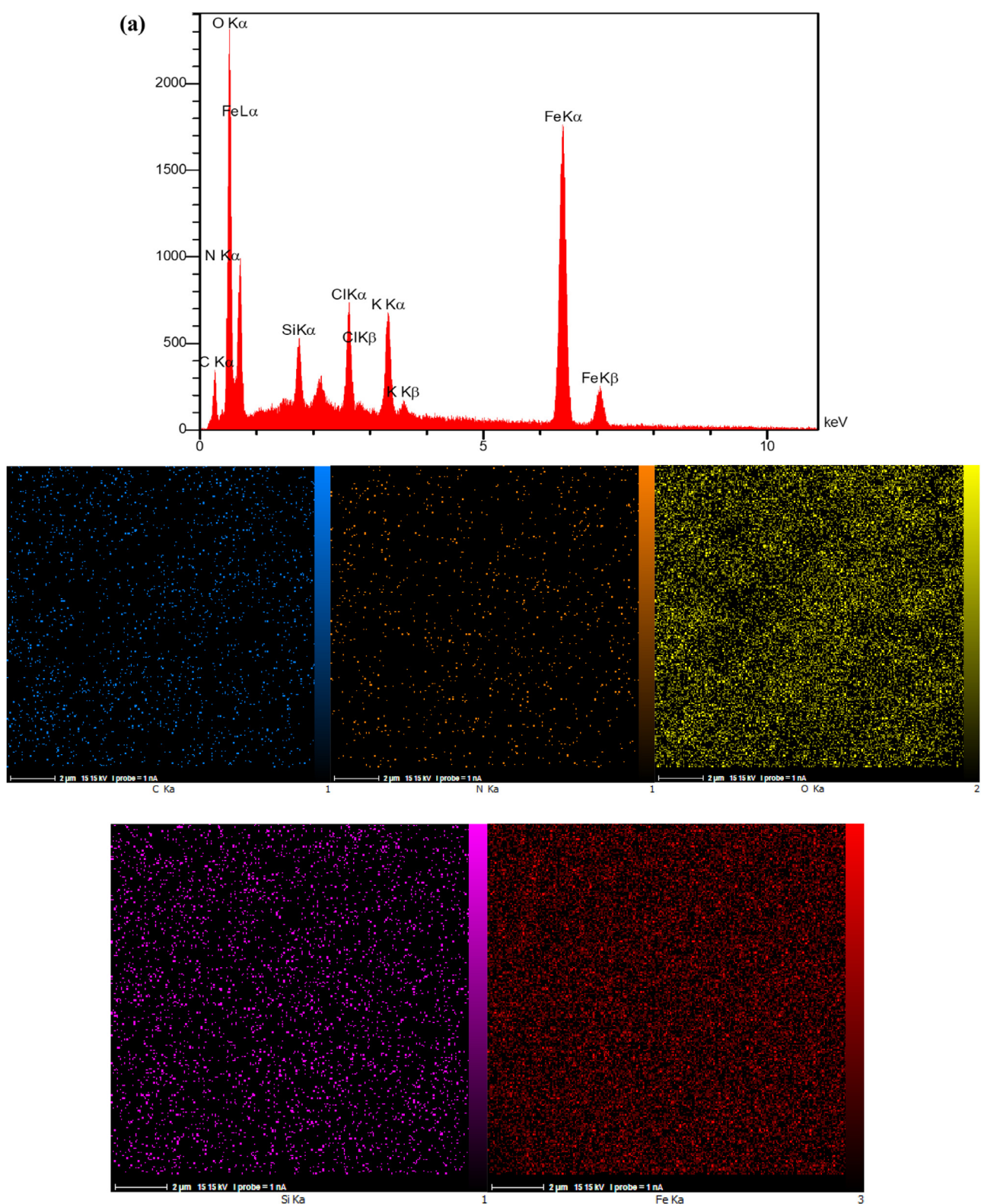


Fig. 2. EDS spectra and elemental mapping of (a)  $\text{Fe}_3\text{O}_4$ -CS@Met and (b)  $\text{Fe}_3\text{O}_4$ -CS@Met-Cu(II).

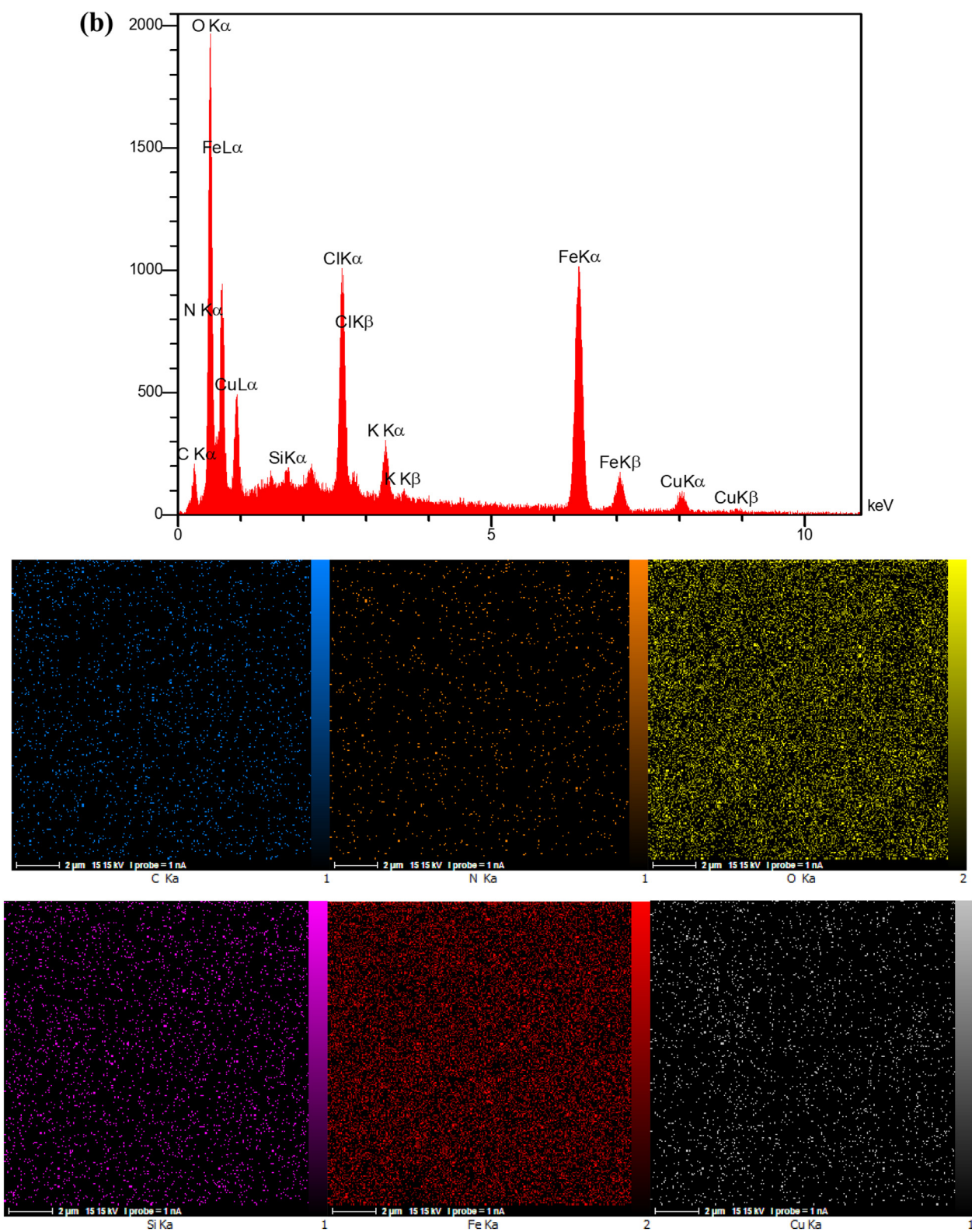


Fig. 2. Continued

diameter is about 13 nm and some nanoparticle aggregations are observed.

Magnetic behavior of the  $\text{Fe}_3\text{O}_4$ -CS@Met-Cu(II) was studied by VSM analysis (Fig. 4). As shown in Fig. 4, the amount of magnetization saturation of  $\text{Fe}_3\text{O}_4$ -CS@Met-Cu(II) is about 30 emu/g. As a result, VSM analysis shows that the nanocatalyst is superparamag-

netic. Magnetic property is the most important advantage of this catalytic system, which causes easy separation from the reaction mixture using an external magnet.

The synthesized  $\text{Fe}_3\text{O}_4$ -CS@Met-Cu(II) catalyst was characterized using FT-IR spectroscopy (Fig. 4). As shown in Fig. 4, the peaks at 3200–3500 and 580  $\text{cm}^{-1}$  are related to NH or OH groups of

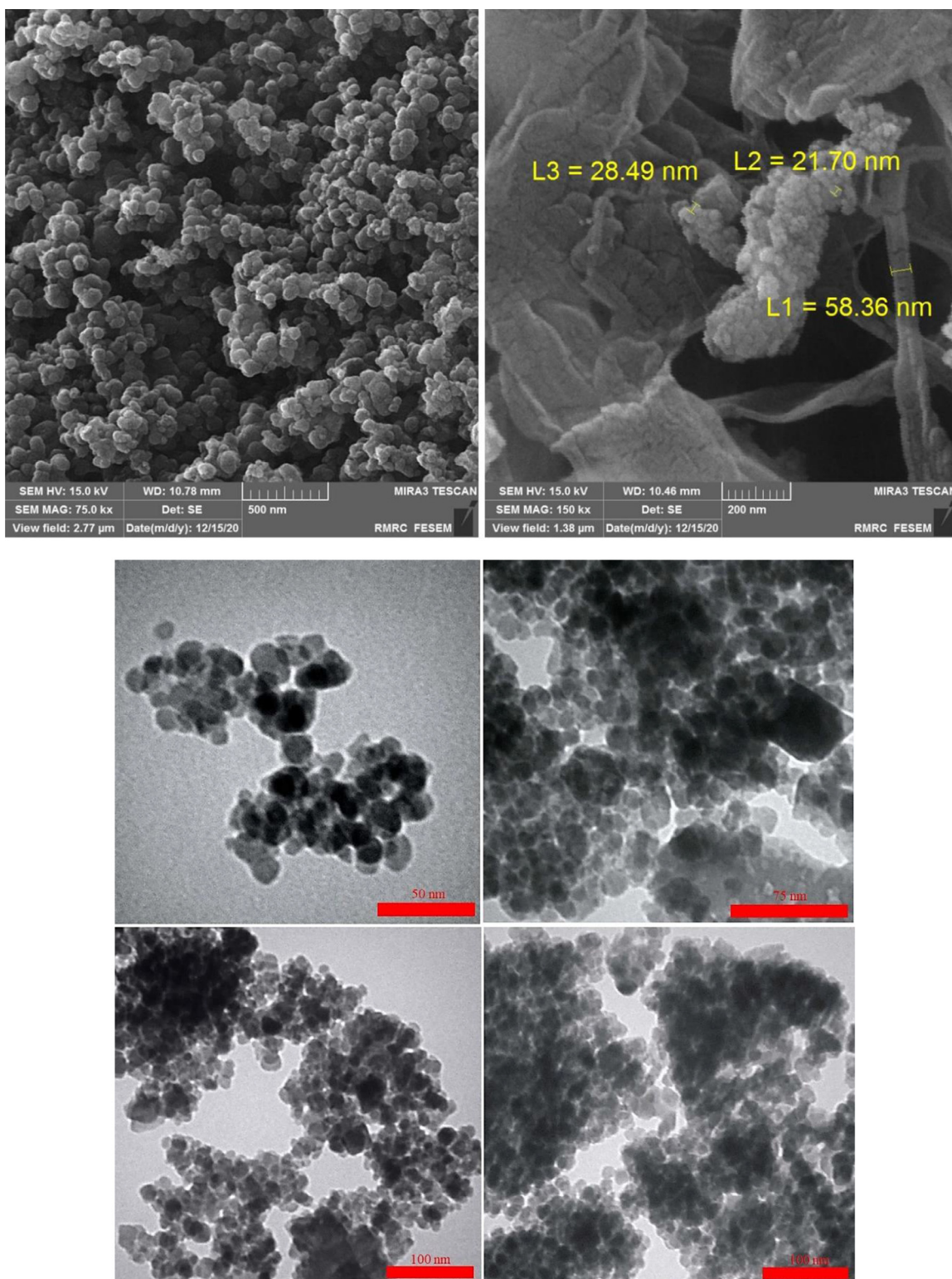


**Fig. 3.** FESEM and TEM images of  $\text{Fe}_3\text{O}_4\text{-CS@Met-Cu(II)}$ .

chitosan and Fe–O groups of  $\text{Fe}_3\text{O}_4$  NPs, respectively, which confirms the presence of magnetic nanoparticles and chitosan. In addition, the peaks in the range of 1640–1690  $\text{cm}^{-1}$  are related to C=N, confirming the presence of metformin in the catalyst struc-

ture. Furthermore, the peaks in 1090 and 790  $\text{cm}^{-1}$  are related to Si–O in the structure of TMOS.

Thermogravimetric analysis (TGA) and differential thermal analysis (DTA) tests in airflow (40 mL/min) at a heating rate of 10  $^{\circ}\text{C}/\text{min}$  on an autonomic TGA-DTG were performed from 25  $^{\circ}\text{C}$

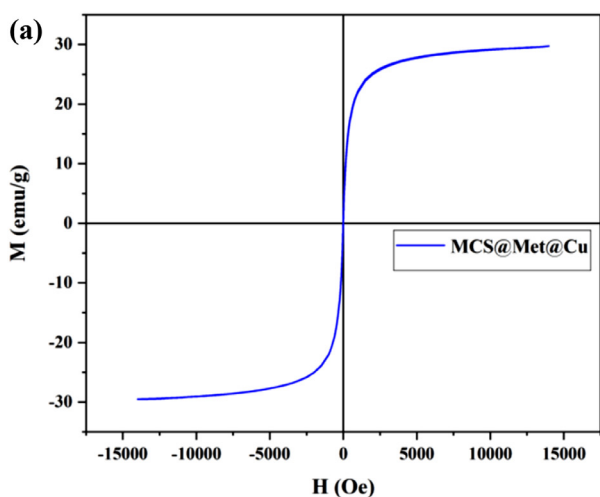


**Fig. 4.** (a) Magnetization curves and (b) FT-IR spectrum of the  $\text{Fe}_3\text{O}_4\text{-CS@Met-Cu(II)}$ .

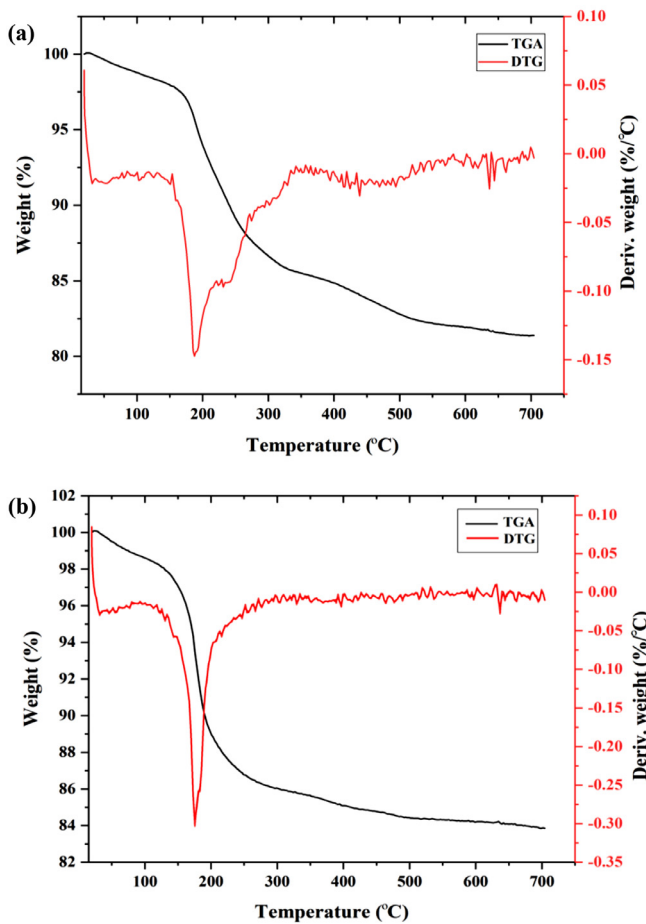
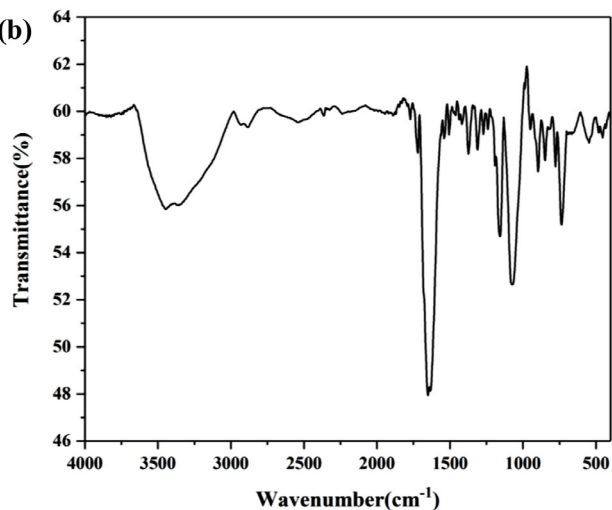


**Fig. 5.** TGA-DTG analysis of (a)  $\text{Fe}_3\text{O}_4\text{-CS@Met}$  and (b)  $\text{Fe}_3\text{O}_4\text{-CS@Met-Cu(II)}$ .

to 700  $^{\circ}\text{C}$ . Fig. 5 (a, b) shows the comparative weight losses of  $\text{Fe}_3\text{O}_4\text{-CS@Met}$  and  $\text{Fe}_3\text{O}_4\text{-CS@Met-Cu(II)}$ , respectively. For both samples, the loss of weight was observed at temperatures below 200  $^{\circ}\text{C}$  due to the release of water and other organic solvents in the structure. In addition, in both cases, the weight loss observed at 200–500  $^{\circ}\text{C}$  was related to the decomposition of chitosan and metformin ligand. As displayed in Fig. 5b, the final decomposition



**Scheme 5.** Proposed mechanism for synthesis of primary sulfonamides.

stage after 600  $^{\circ}\text{C}$  corresponds to the decomposition of the synthesized  $\text{Fe}_3\text{O}_4\text{-CS@Met-Cu(II)}$ .

### 3.2. Ultrasound-mediated synthesis of primary sulfonamides

Primary sulfonamides were synthesized via the reaction of sodium cyanate (10 mmol) and aryl sulfonyl chlorides (10 mmol) in  $\text{H}_2\text{O}$  (50 mL) as the solvent under ultrasonic irradiation for 20 min (Table 1). The proposed mechanism is displayed in Table 1. As presented in Scheme 5, water has been used as a solvent and nucleophile [57]. Since stoichiometric quantities of the substrates are used up after the reaction is complete, there are no substrates left and the only side product formed is  $\text{NaCl}$  salt.

### 3.3. N-Arylation of primary sulfonamides

$\text{Fe}_3\text{O}_4\text{-CS@Met-Cu(II)}$  was applied as a magnetic nanocatalyst for *N*-arylation of primary sulfonamides with arylboronic acids in ethanol under reflux conditions. The reaction conditions for *N*-arylation of *p*-toluenesulfonamide ( $p\text{-TsNH}_2$ ) using  $\text{PhB(OH)}_2$  were optimized using different amounts of catalyst and bases in ethanol (Table 2). In the absence of catalyst or base in the reaction, no reaction takes place (Table 2, entries 1 and 2). The results indicate that the presence of  $\text{Fe}_3\text{O}_4\text{-CS@Met-Cu(II)}$  and the base is required for *N*-arylation of sulfonamides. Among the various bases used in the reaction, trimethylamine ( $\text{Et}_3\text{N}$ ) was found the best (Table 2,

**Table 1**

Synthesis of primary sulfonamides.

Entry	Substrate	Product	Yield (%) <sup>a</sup>	Melting point (°C)	Melting point (°C) [lit.]
1			98	136-138	136-140 [58]
2			95	140-144	140-144 [Aldrich]
3			94	150-151	149-152 [Aldrich]
4			90	179-181	178-180 [Aldrich]
5			95	164-166	163-167 [Aldrich]

<sup>a</sup> Isolated yield.**Table 2**  
Optimization of the reaction conditions.<sup>a</sup>

Entry	Fe <sub>3</sub> O <sub>4</sub> -CS@Met-Cu(II) (g)	Base	Time (min)	Yield (%) <sup>b</sup>
1	0.0	-	40	0.0
2	0.0	Et <sub>3</sub> N	40	0.0
3	0.01	K <sub>2</sub> CO <sub>3</sub>	50	75
4	0.01	Et <sub>3</sub> N	30	86
5	0.01	Na <sub>2</sub> CO <sub>3</sub>	50	70
6	0.015	K <sub>2</sub> CO <sub>3</sub>	55	83
7	0.02	K <sub>2</sub> CO <sub>3</sub>	25	85
8	0.02	Na <sub>2</sub> CO <sub>3</sub>	35	75
9	0.02	Et <sub>3</sub> N	20	95

<sup>a</sup> Reaction conditions: Phenylboronic acid (0.5 mmol), *p*-TsNH<sub>2</sub> (0.5 mmol), base (0.7 mmol), catalyst, ethanol (7 mL), reflux.

<sup>b</sup> Isolated yield.

entry 9). The product yield increased when the catalyst amount increased to 0.01 g. According to the results, the optimal amount of the catalyst is 0.02 g (Table 2, entry 9). On the other hand, decreasing the catalyst loading will cause the reaction to be incomplete (Table 2, entry 4).

After optimizing the reaction conditions, various primary sulfonamides with electron withdrawing and donating groups and a wide range of arylboronic acids were examined to synthesize the secondary sulfonamides (Table 3). In all cases, the products were synthesized in high yields. The results indicate that *ortho*-substituted arylboronic acids react slowly compared to *para* isomers (Table 3, entries 3 and 6). However, electronic effects do not play much of a role in the product yields.

The melting points of all the products were recorded and compared with those of authentic samples [13]. The FT-IR and <sup>1</sup>H NMR spectra also confirm the structure of products (Figure S1-S3, see Supporting Information). The appearance of the two strong and sharp absorption bands in the structure of primary sulfonamides (NH<sub>2</sub> stretching bands) and the disappearance of one absorption band (NH stretching vibration) confirm the formation of the secondary sulfonamides (Figure S1).

The efficacy and capability of our catalyst were compared with those of some reported catalysts in *N*-arylation of 4-

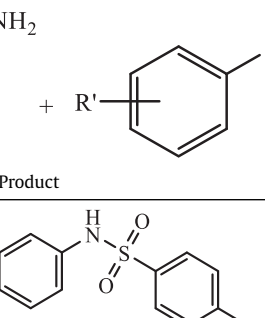
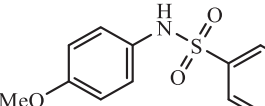
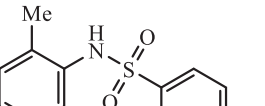
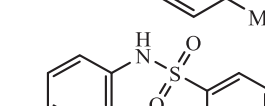
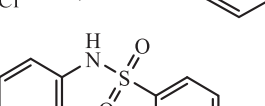
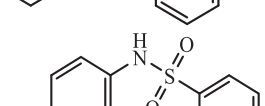
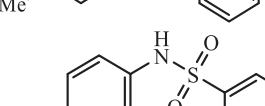
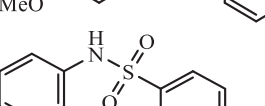
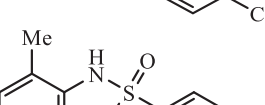
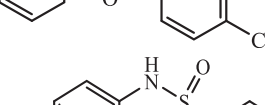
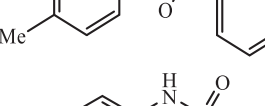
methylbenzenesulfonamides, as summarized in Table 4. Fe<sub>3</sub>O<sub>4</sub>-CS@Met-Cu(II) nanocatalyst was observed to be an efficient catalyst due to the reasonable reaction time, ease of operation, simplicity of simple work-up protocol, and reaction conditions. In addition, compared to other catalysts, Fe<sub>3</sub>O<sub>4</sub>-CS@Met-Cu(II) nanocatalyst can be easily separated from the reaction mixture by a magnet and reused in several consecutive cycles.

**3.4 Possible mechanism for *N*-arylation of primary sulfonamides** A catalytic cycle mechanism is proposed for the *N*-arylation reaction of primary sulfonamides using Fe<sub>3</sub>O<sub>4</sub>-CS@Met-Cu(II) in the presence of Et<sub>3</sub>N as an appropriate base (Scheme 6). As observed in Scheme 6, the oxidative addition reaction of the catalyst occurs in the first stage, leading to the formation of an intermediate (a). In the second stage, the reaction occurs between deprotonated primary sulfonamides and intermediate (a) by nucleophilic attack. Finally, the formation of the desired product and the regeneration of the catalyst are carried out by a reductive elimination stage.

#### 3.4. Reusability of Fe<sub>3</sub>O<sub>4</sub>-CS@Met-Cu(II)

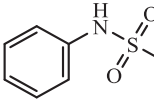
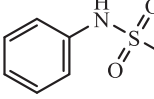
One of the most important features of a catalyst is the ability to recycle and reuse it. The recyclability of the Fe<sub>3</sub>O<sub>4</sub>-CS@Met-Cu(II) was studied in a model reaction of *p*-TsNH<sub>2</sub> and phenylboronic acid in the presence of Et<sub>3</sub>N as an effective base in EtOH solvent. When the reaction was complete, the catalyst was removed from the reaction mixture using a magnet and reused in the next cycles. The synthesized magnetic catalyst can be applied 5 times with no considerable loss of catalytic performance (Fig. 6). Fig. 7 displays the FT-IR, XRD, and VSM analyses of the recycled catalyst. As observed in Fig. 7a, in contrast to the fresh catalyst, the FT-IR spectrum of the recycled catalyst has all the peaks related to C=N, NH or OH, Fe-O, and Si-O groups, in 1640-1690, 3200-3500, 580, and 1090 and 790 cm<sup>-1</sup>, respectively. According to Fig. 7b, the XRD pattern of the recycled catalyst shows the same peaks as in the fresh catalyst. Moreover, copper leaching investigation of the catalyst after the recycling tests by ICP-MS analysis was found to be negligible (~0.1%). In addition, Fig. 7c shows the VSM analysis of

**Table 3***N*-Arylation of primary sulfonamides with arylboronic acids in ethanol.<sup>a</sup>

Entry	R	R'	Product			Melting point (°C) (lit. m.p. [Ref.])	TON	TOF (min <sup>-1</sup> )
				Time (min)	Yield (%) <sup>b</sup>			
1	4-Me	H		20	95	100-103 (102-103 [59])	33181	1659
2	4-Me	4-OMe		35	91	113-114 (112-114 [60])	31784	908
3	4-Me	2-Me		50	90	107-109 (105-107 [59])	31435	628
4	4-Me	4-Cl		30	90	118-122 (118-119 [59])	31435	1047
5	H	H		30	90	109-111 (110 [Aldrich])	31435	1047
6	H	4-Me		35	90	120-122 (117-119 [61])	31435	898
7	H	4-OMe		35	89	97-100 (93-94.5 [62])	31086	888
8	4-Cl	H		30	91	102-104 (104-105 [59])	31784	1059
9	4-Cl	2-Me		50	87	106-110 (-)	30387	607
10	4-Cl	4-Me		40	90	84-86 ([commercial])	31435	785
11	4-Cl	4-OMe		40	88	140-144 (141-142 [59])	30736	768

(continued on next page)

**Table 3** (continued)

Entry	R	R'	Product	Time (min)	Yield (%) <sup>b</sup>	Melting point (°C) (lit. m.p. [Ref.])	TON	TOF (min <sup>-1</sup> )
12	4-Br	H		70	80	115-117 (116-117 [63])	27942	349
13	4-NO <sub>2</sub>	H		90	75	134-137 (135-136 [59])	26196	291

<sup>a</sup> Reaction conditions: Arylboronic acid (0.5 mmol), sulfonamide (0.5 mmol), Et<sub>3</sub>N (0.7 mmol), Fe<sub>3</sub>O<sub>4</sub>-CS@Met-Cu(II) (0.02 g), EtOH (7 mL), reflux.

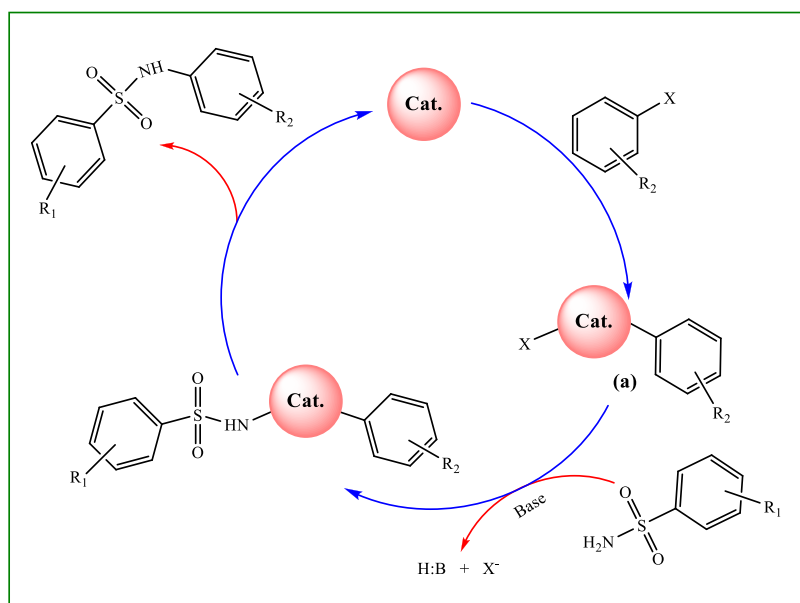
<sup>b</sup> Isolated yield.

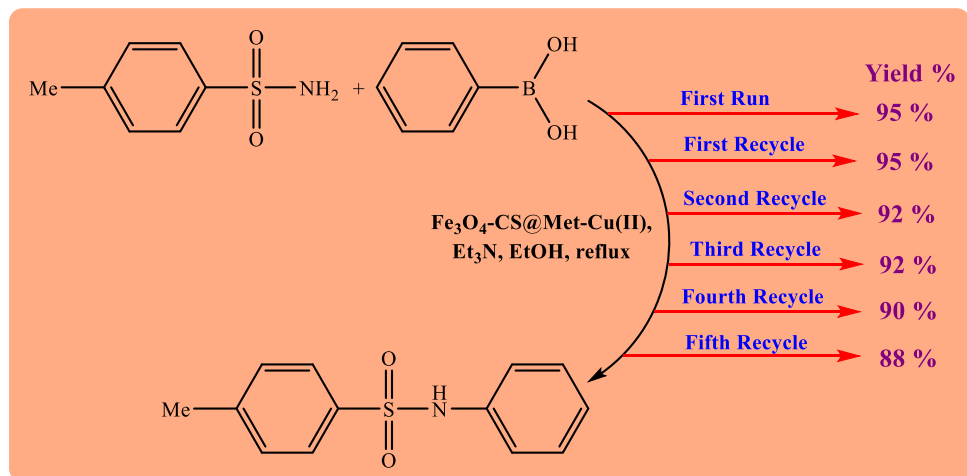
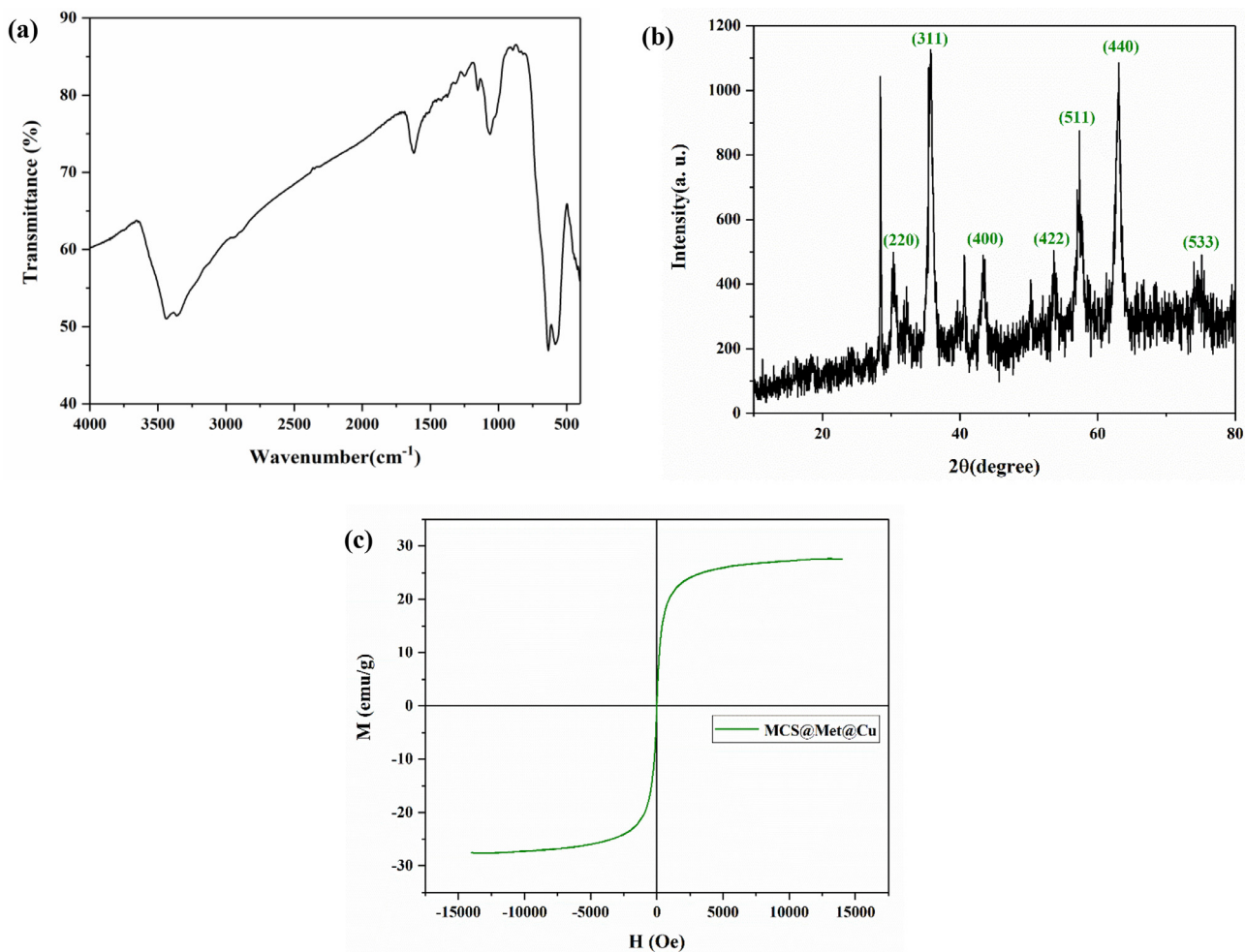
**Table 4**

Comparison of Fe<sub>3</sub>O<sub>4</sub>-CS@Met-Cu(II) nanocatalyst with other reported catalysts in the *N*-arylation of 4-methylbenzenesulfonamides.

Entry	Catalyst	Substrate	Reaction condition	Time	Yield (%) <sup>a</sup>	Ref.
1	Cu(OAc) <sub>2</sub>	Phenylboronic acid	Dry isopropanol, K <sub>2</sub> CO <sub>3</sub> , 90 °C in a sealed tube	12 h	65	[8]
2	CuI	Phenyl bromide	K <sub>2</sub> CO <sub>3</sub> , microwave heating	3 h	70	[10]
3	CuI/ <i>N</i> -methylglycine	Phenyl iodide	DMF, K <sub>3</sub> PO <sub>4</sub>	-	95	[14]
4	Cu-zeolite NPs	Phenylboronic acid	K <sub>2</sub> CO <sub>3</sub> , H <sub>2</sub> O, reflux	3 h	95	[57]
5	Mn/Cu cocatalyzed	Phenyl iodide	CuI, MnF <sub>2</sub> , DMEDA, KOH, H <sub>2</sub> O, 60 °C	24 h	97	[18]
6	Cu(OAc) <sub>2</sub> .H <sub>2</sub> O	Phenylboronic acid	Anhyd. MeOH, reflux	-	50	[64]
7	Fe <sub>3</sub> O <sub>4</sub> -CS@Met-Cu(II)	Phenylboronic acid	Et <sub>3</sub> N, EtOH, reflux	20 min	95	This work

<sup>a</sup> Isolated yield.

**Scheme 6.** Proposed mechanism for *N*-arylation of primary sulfonamides.

**Fig. 6.** Reusability of  $\text{Fe}_3\text{O}_4\text{-CS@Met-Cu(II)}$  in *N*-arylation of  $p\text{-TsNH}_2$ .**Fig. 7.** (a) FT-IR, (b) XRD, and (c) VSM analysis of the recycled catalyst.

the recycled catalyst, which indicates that the recycled catalyst has significant magnetic properties.

#### 4. Conclusion

In conclusion, a green and easy technique has been developed for the preparation of primary sulfonamides under ultrasonic irradiation. An efficient and magnetic nanocatalyst based on chitosan

( $\text{Fe}_3\text{O}_4\text{-CS@Met-Cu(II)}$ ) has then been synthesized and applied in the *N*-arylation of different primary sulfonamides with arylboronic acids in ethanol under reflux conditions. In this study, chitosan was applied as an efficient, natural, and novel support to synthesize a heterogeneous catalyst.  $\text{Fe}_3\text{O}_4\text{-CS@Met-Cu(II)}$  was characterized using different analytical methods including XRD, TEM, FE-SEM, EDS, elemental mapping, VSM, ICP-MS, TGA/DTG, and FT-IR. The experimental results show the high catalytic performance of

$\text{Fe}_3\text{O}_4$ -CS@Met-Cu(II) and the formation of the products in high yields. Finally,  $\text{Fe}_3\text{O}_4$ -CS@Met-Cu(II) can be recycled 5 times without any important reduction in its performance, which shows its high stability.

### Declaration of Competing Interest

The authors declare that they have no known competing financial interests or personal relationships that could have appeared to influence the work reported in this paper.

### Acknowledgments

We gratefully acknowledge the University of Qom for the support of this work.

### Supplementary materials

Supplementary material associated with this article can be found, in the online version, at doi:[10.1016/j.jorgchem.2021.121915](https://doi.org/10.1016/j.jorgchem.2021.121915).

### References

- [1] J. Choi, P. Martín-Gago, G.C. Fu, Stereoconvergent arylations and alkylations of unactivated alkyl electrophiles: catalytic enantioselective synthesis of secondary sulfonamides and sulfones, *J. Am. Chem. Soc.* 136 (2014) 12161–12165.
- [2] I. Nishimori, T. Minakuchi, K. Morimoto, S. Sano, S. Onishi, H. Takeuchi, D. Vullo, A. Scozzafava, C.T. Supuran, Carbonic anhydrase inhibitors: DNA cloning and inhibition studies of the  $\alpha$ -carbonic anhydrase from Helicobacter pylori, a new target for developing sulfonamide and sulfamate gastric drugs, *J. Med. Chem.* 49 (2006) 2117–2126.
- [3] S. Caddick, J.D. Wilden, H.D. Bush, S.N. Wadman, D.B. Judd, A new route to sulfonamides via intermolecular radical addition to pentafluorophenyl vinylsulfonate and subsequent aminolysis, *Org. Lett.* 4 (2002) 2549–2551.
- [4] P.R. Hanson, D.A. Probst, R.E. Robinson, M. Yau, Cyclic sulfonamides via the ring-closing metathesis reaction, *Tetrahedron Lett.* 40 (1999) 4761–4764.
- [5] L. De Luca, G. Giacomelli, An easy microwave-assisted synthesis of sulfonamides directly from sulfonic acids, *J. Org. Chem.* 73 (2008) 3967–3969.
- [6] X. Cao, Y. Bai, Y. Xie, G.-J. Deng, Palladium-catalyzed arylation of aryl sulfonamides with cyclohexanones, *J. Mol. Catal. A Chem.* 383 (2014) 94–100.
- [7] S. Shekhar, T.B. Dunn, B.J. Kotecki, D.K. Montavon, S.C. Cullen, A general method for palladium-catalyzed reactions of primary sulfonamides with aryl naphthalenes, *J. Org. Chem.* 76 (2011) 4552–4563.
- [8] C. Pan, J. Cheng, H. Wu, J. Ding, M. Liu, Cu(OAc)<sub>2</sub>-catalyzed *N*-arylation of sulfonamides with arylboronic acids or trimethoxy (phenyl) silane, *Synth. Commun.* 39 (2009) 2082–2092.
- [9] M.L. Kantam, B. Neelima, C.V. Reddy, V. Neeraja, *N*-Arylation of imidazoles, imides, amines, amides and sulfonamides with boronic acids using a recyclable Cu(OAc)<sub>2</sub>-H<sub>2</sub>O/[bmim][BF<sub>4</sub>] system, *J. Mol. Catal. A Chem.* 249 (2006) 201–206.
- [10] H. He, Y.-J. Wu, Copper-catalyzed *N*-arylation of sulfonamides with aryl bromides and iodides using microwave heating, *Tetrahedron Lett.* 44 (2003) 3385–3386.
- [11] G. Burton, P. Cao, G. Li, R. Rivero, Palladium-catalyzed intermolecular coupling of aryl chlorides and sulfonamides under microwave irradiation, *Org. Lett.* 5 (2003) 4373–4376.
- [12] T. Ikawa, T.E. Barder, M.R. Biscoe, S.L. Buchwald, Pd-catalyzed amidations of aryl chlorides using monodentate biaryl phosphine ligands: A kinetic, computational, and synthetic investigation, *J. Am. Chem. Soc.* 129 (2007) 13001–13007.
- [13] Y. Orooji, K. Pakzad, M. Nasrollahzadeh, M. Tajbakhsh, Novel magnetic lignosulfonate-supported Pd complex as an efficient nanocatalyst for *N*-arylation of 4-methylbenzenesulfonamide, *Int. J. Biol. Macromol.* 182 (2021) 564–573.
- [14] W. Deng, L. Liu, C. Zhang, M. Liu, Q.-X. Guo, Copper-catalyzed cross-coupling of sulfonamides with aryl iodides and bromides facilitated by amino acid ligands, *Tetrahedron Lett.* 46 (2005) 7295–7298.
- [15] Y.-Q. Ouyang, Z.-H. Yang, Z.-H. Chen, S.-Y. Zhao, Efficient copper-catalyzed *N*-arylation of NH-containing heterocycles and sulfonamides with arenediazonium tetrafluoroborates, *Synth. Commun.* 47 (2017) 771–778.
- [16] W. Zu, S. Liu, X. Jia, L. Xu, Chemoselective *N*-arylation of aminobenzene sulfonamides via copper catalysed Chan-Evans-Lam reactions, *Org. Chem. Front.* 6 (2019) 1356–1360.
- [17] Z.-G. Zheng, J. Wen, N. Wang, B. Wu, X.-Q. Yu, *N*-Arylation of amines, amides, imides and sulfonamides with arylboroxines catalyzed by simple copper salt/EtOH system, *Beilstein J. Org. Chem.* 4 (2008) 40.
- [18] Y. Teo, F. Yong, I.K. Ithnin, S.T. Yio, Z. Lin, Efficient manganese/copper bimetallic catalyst for *N*-arylation of amides and sulfonamides under mild conditions in water, *Eur. J. Org. Chem.* 2013 (2013) 515–524.
- [19] W.F. Paxton, J.M. Spruell, J.F. Stoddart, Heterogeneous catalysis of a copper-coated atomic force microscopy tip for direct-write click chemistry, *J. Am. Chem. Soc.* 131 (2009) 6692–6694.
- [20] M. Behrens, Heterogeneous catalysis of CO<sub>2</sub> conversion to methanol on copper surfaces, *Angew. Chemie Int. Ed.* 53 (2014) 12022–12024.
- [21] Z. Nezafat, M. Nasrollahzadeh, Biosynthesis of Cu/Fe<sub>3</sub>O<sub>4</sub> nanoparticles using *Alhagi camelorum* aqueous extract and their catalytic activity in the synthesis of 2-imino-3-aryl-2, 3-dihydrobenzo [d] oxazol-5-ol derivatives, *J. Mol. Struct.* (2020) 129731.
- [22] M. Nasrollahzadeh, S.M. Sajadi, Preparation of Pd/Fe<sub>3</sub>O<sub>4</sub> nanoparticles by use of *Euphorbia stracheyi* Boiss root extract: a magnetically recoverable catalyst for one-pot reductive amination of aldehydes at room temperature, *J. Colloid Interface Sci.* 464 (2016) 147–152.
- [23] N. Kerru, S.V.H.S. Bhaskaruni, L. Gummidi, S.N. Maddila, S. Maddila, S.B. Jonnalagadda, Recent advances in heterogeneous catalysts for the synthesis of imidazole derivatives, *Synth. Commun.* 49 (2019) 2437–2459.
- [24] M. Mohammadi, A. Ghorbani-Choghamarani, L-Methionine-Pd complex supported on hencryst as a highly efficient and reusable nanocatalyst for C-C cross-coupling reactions, *New J. Chem.* 44 (2020) 2919–2929.
- [25] J. Zhao, X. Yang, W. Wang, J. Liang, Y. Orooji, C. Dai, X. Fu, Y. Yang, W. Xu, J. Zhu, Efficient sorbitol producing process through glucose hydrogenation catalyzed by Ru supported amino poly(styrene-co-maleic) polymer (ASMA) encapsulated on  $\gamma$ -Al<sub>2</sub>O<sub>3</sub>, *Catalysts* 10 (9) (2020) 1068.
- [26] A. Omidvar, M.R. Rashidian Vaziri, B. Jaleh, N.P. Shabestari, M. Noroozi, Metal-enhanced fluorescence of graphene oxide by palladium nanoparticles in the blue-green part of the spectrum, *Chin. Phys. B* 25 (11) (2016) 118102.
- [27] Y. Cheng, Y. Fan, Y. Pei, M. Qiao, Graphene-supported metal/metal oxide nanohybrids: synthesis and applications in heterogeneous catalysis, *Catal. Sci. Technol.* 5 (2015) 3903–3916.
- [28] M. Trueba, S.P. Trasatti,  $\gamma$ -Alumina as a support for catalysts: a review of fundamental aspects, *Eur. J. Inorg. Chem.* 2005 (2005) 3393–3403.
- [29] Z. Taherian, A. Khataee, Y. Orooji, Facile synthesis of yttria-promoted nickel catalysts supported on MgO-MCM-41 for syngas production from greenhouse gases, *Renew. Sust. Energ. Rev.* 134 (2020) 110130.
- [30] Y. Zhang, B.Y.W. Hsu, C. Ren, X. Li, J. Wang, Silica-based nanocapsules: synthesis, structure control and biomedical applications, *Chem. Soc. Rev.* 44 (2015) 315–335.
- [31] Y. Orooji, B. Jaleh, F. Homayouni, P. Fakhri, M. Kashfi, M.J. Torkamany, A.A. Yousefi, Laser ablation-assisted synthesis of poly(vinylidene fluoride)/Au nanocomposites: crystalline phase and micromechanical finite element analysis, *Polymers* 12 (11) (2020) 2630.
- [32] G. Martínez-Edo, A. Balmori, I. Pontón, A. Martí del Rio, D. Sánchez-García, Functionalized ordered mesoporous silicas (MCM-41): Synthesis and applications in catalysis, *Catalysts* 8 (2018) 617.
- [33] M. Mohammadi, M. Khodamorady, B. Tahmasbi, K. Bahrami, A. Ghorbani-Choghamarani, Boehmite nanoparticles as versatile support for organic-inorganic hybrid materials: synthesis, functionalization, and applications in eco-friendly catalysis, *J. Ind. Eng. Chem.* (2021).
- [34] S. Singh, R. Kumar, H.D. Setiabudi, S. Nanda, D.-V.N. Vo, Advanced synthesis strategies of mesoporous SBA-15 supported catalysts for catalytic reforming applications: a state-of-the-art review, *Appl. Catal. A Gen.* 559 (2018) 57–74.
- [35] S. Yuan, M. Wang, J. Liu, B. Guo, Recent advances of SBA-15-based composites as the heterogeneous catalysts in water decontamination: a mini-review, *J. Environ. Manage.* 254 (2020) 109787.
- [36] P. Verma, Y. Kuwahara, K. Mori, R. Raja, H. Yamashita, Functionalized mesoporous SBA-15 silica: recent trends and catalytic applications, *Nanoscale* 12 (2020) 11333–11363.
- [37] Y. Orooji, S. Mortazavi-Derazkola, S.M. Ghoreishi, M. Amiri, M. Salavati-Niasari, Mesoporous Fe<sub>3</sub>O<sub>4</sub>@SiO<sub>2</sub>-hydroxyapatite nanocomposite: reen sonochemical synthesis using strawberry fruit extract as a capping agent, characterization and their application in sulfasalazine delivery and cytotoxicity, *J. Hazard. Mater.* 400 (2020) 123140.
- [38] T. Baran, Pd NPs@Fe<sub>3</sub>O<sub>4</sub>/chitosan/pumice hybrid beads: A highly active, magnetically retrievable, and reusable nanocatalyst for cyanation of aryl halides, *Carbohydr. Polym.* 237 (2020) 116105.
- [39] R.W. Murray, Nanoelectrochemistry: metal nanoparticles, nanoelectrodes, and nanopores, *Chem. Rev.* 108 (2008) 2688–2720.
- [40] J. Sun, J. Wang, W. Cheng, J. Zhang, X. Li, S. Zhang, Y. She, Chitosan functionalized ionic liquid as a recyclable biopolymer-supported catalyst for cycloaddition of CO<sub>2</sub>, *Green Chem.* 14 (2012) 654–660.
- [41] M. Chtchigrovsky, A. Primo, P. Gonzalez, K. Molvinger, M. Robitzer, F. Quignard, F. Taras, Functionalized chitosan as a green, recyclable, biopolymer-supported catalyst for the [3+ 2] Huisgen cycloaddition, *Angew. Chemie Int. Ed.* 48 (2009) 5916–5920.
- [42] S. Chairam, W. Konkamdee, R. Parakhun, Starch-supported gold nanoparticles and their use in 4-nitrophenol reduction, *J. Saudi Chem. Soc.* 21 (2017) 656–663.
- [43] T. Baran, Practical, economical, and eco-friendly starch-supported palladium catalyst for Suzuki coupling reactions, *J. Colloid Interface Sci.* 496 (2017) 446–455.
- [44] M. Nasrollahzadeh, N. Shafiei, Z. Nezafat, N.S.S. Bidgoli, F. Soleimani, Recent progresses in the application of cellulose, starch, alginate, gum, pectin, chitin and chitosan based (nano) catalysts in sustainable and selective oxidation reactions: A review, *Carbohydr. Polym.* (2020) 116353.

- [45] M. Chen, H. Kang, Y. Gong, J. Guo, H. Zhang, R. Liu, Bacterial cellulose supported gold nanoparticles with excellent catalytic properties, *ACS Appl. Mater. Interfaces* 7 (2015) 21717–21726.
- [46] S. Ahmed, S. Ahmed, S. Ikram, Chitin and chitosan: history, composition and properties, *Chitosan Deriv. Compos. Appl.* (2017) 1–24.
- [47] S. Ahmed, S. Ikram, Chitosan & its derivatives: a review in recent innovations, *Int. J. Pharm. Sci. Res.* 6 (2015) 14.
- [48] S.M. Anush, H.R. Chandan, B.H. Gayathri, N. Manju, B. Vishalakshi, B. Kalluraya, Graphene oxide functionalized chitosan-magnetic nanocomposite for removal of Cu(II) and Cr(VI) from waste water, *Int. J. Biol. Macromol.* 164 (2020) 4391–4402.
- [49] S.M. Anush, B. Vishalakshi, B. Kalluraya, N. Manju, Synthesis of pyrazole-based Schiff bases of Chitosan: Evaluation of antimicrobial activity, *Int. J. Biol. Macromol.* 119 (2018) 446–452.
- [50] T. Wang, Y. Luo, Chitosan hydrogel beads functionalized with thymol-loaded solid lipid-polymer hybrid nanoparticles, *Int. J. Mol. Sci.* 19 (2018) 3112.
- [51] T. Baran, A. Menteş, Microwave assisted synthesis of biaryl by CC coupling reactions with a new chitosan supported Pd(II) catalyst, *J. Mol. Struct.* 1122 (2016) 111–116.
- [52] M. Nasrollahzadeh, M. Sajjadi, M. Shokouhimehr, R.S. Varma, Recent developments in palladium (nano)catalysts supported on polymers for selective and sustainable oxidation processes, *Coord. Chem. Rev.* 397 (2019) 54–75.
- [53] S. Fortun, P. Beauclair, A.R. Schmitzer, Metformin as a versatile ligand for recyclable palladium-catalyzed cross-coupling reactions in neat water, *RSC Adv.* 7 (2017) 21036–21044.
- [54] P. Yang, R. Ma, F. Bian, Palladium supported on metformin-functionalized magnetic polymer nanocomposites: A highly efficient and reusable catalyst for the Suzuki-Miyaura coupling reaction, *ChemCatChem.* 8 (24) (2016) 3746–3754.
- [55] A.S. Hamed, E.M. Ali, Cu(II)-metformin immobilized on graphene oxide: an efficient and recyclable catalyst for the Beckmann rearrangement, *Res. Chem. Intermed.* 46 (2020) 701–714.
- [56] A. Soozanipour, A. Taheri-Kafrani, M. Barkhori, M. Nasrollahzadeh, Preparation of a stable and robust nanobiocatalyst by efficiently immobilizing of pectinase onto cyanuric chloride-functionalized chitosan grafted magnetic nanoparticles, *J. Colloid Interface Sci.* 536 (2019) 261–270.
- [57] D. Azarifar, F. Soleimanei, Natural Indian Natrolite zeolite-supported Cu nanoparticles: a new and reusable heterogeneous catalyst for *N*-arylation of sulfonamides with boronic acids in water under ligand-free conditions, *RSC Adv.* 4 (2014) 12119–12126.
- [58] F. Rolla, Sodium borohydride reactions under phase-transfer conditions: reduction of azides to amines, *J. Org. Chem.* 47 (1982) 4327–4329.
- [59] C. You, F. Yao, T. Yan, M. Cai, A highly efficient heterogeneous copper-catalyzed Chan-Lam coupling reaction of sulfonyl azides with arylboronic acids leading to *N*-arylsulfonamides, *RSC Adv.* 6 (2016) 43605–43612.
- [60] Y.-C. Teo, F.-F. Yong, Efficient ligand-free, copper-catalyzed *N*-arylation of sulfonamides, *Synlett* 2011 (2011) 837.
- [61] M.Z.A. Badr, M.M. Aly, A.M. Fahmy, Molecular rearrangements. 19. Thermolysis and photolysis of *N*-arylbzenenesulfonamides, *J. Org. Chem.* 46 (1981) 4784–4787.
- [62] R. Hosseinzadeh, M. Tajbakhsh, M. Mohadjerani, M. Alikarami, Copper-catalysed *N*-arylation of arylsulfonamides with aryl bromides and aryl iodides using KF/Al<sub>2</sub>O<sub>3</sub>, *J. Chem. Sci.* 122 (2010) 143–148.
- [63] W. Zhang, J. Xie, B. Rao, M. Luo, Iron-catalyzed *N*-arylsulfonamide formation through directly using nitroarenes as nitrogen sources, *J. Org. Chem.* 80 (2015) 3504–3511.
- [64] J.-B. Lan, G.-L. Zhang, X.-Q. Yu, J.-S. You, L. Chen, M. Yan, R.-G. Xie, A simple copper salt catalyzed *N*-arylation of amines, amides, imides, and sulfonamides with arylboronic acids, *Synlett* 2004 (2004) 1095–1097.